Unclassified

SEC

AD-A201 969

ORT DOCUMENTATION PAGE

1a

1b RESTRICTIVE MARKINGS

2a

3 DISTRIBUTION / AVAILABILITY OF REPORT
Approved for public release; Distribution Unlimited.

2b DECLASSIFICATION / DOWNGRADING SCHEDULE

4. PERFORMING ORGANIZATION REPORT NUMBER(S)
AFGL-TR-88-0316

5. MONITORING ORGANIZATION REPORT NUMBER(S)

6a NAME OF PERFORMING ORGANIZATION	6b OFFICE SYMBOL (If applicable)	7a NAME OF MONITO ORGANIZATION
Air Force Geophysics Laboratory	LYR	

6c. ADDRESS (City, State, and ZIP Code)	7b ADDRESS (City, S d ZIP Code)
Hanscom AFB Massachusetts 01731-5000	

8a. NAME OF FUNDING / SPONSORING ORGANIZATION	8b OFFICE SYMBOL (If applicable)	9 PROCUREMENT INSTRUMENT IDENTIFICATION NUMBER

8c. ADDRESS (City, State, and ZIP Code)	10 SOURCE OF FUNDING NUMBERS			
	PROGRAM ELEMENT NO	PROJECT NO	TASK NO	WORK UNIT ACCESSION NO
	61102F	2310	G8	03

11 TITLE (Include Security Classification)
A New Slant on the Distribution and Measurement of Hydrometeor Canting Angles

12 PERSONAL AUTHOR(S)
James I. Metcalf

13a TYPE OF REPORT	13b TIME COVERED	14 DATE OF REPORT (Year, Month, Day)	15 PAGE COUNT
Reprint	FROM _____ TO _____	1988 November 23	8

16 SUPPLEMENTARY NOTATION
Reprinted from Journal of Atmospheric and Oceanic Technology, Vol. 5, No. 4, August 1988

17 COSATI CODES			18 SUBJECT TERMS (Continue on reverse if necessary and identify by block number)
FIELD	GROUP	SUB-GROUP	Canting angle, Polarization diversity radar, Hydrometeor

19 ABSTRACT (Continue on reverse if necessary and identify by block number)

Several models have been developed in the past to describe the distribution of hydrometeor canting angles and the resulting effects on polarimetric radar measurements. These models are reviewed to compare their characteristics and to assess their validity under specified conditions. Of particular interest is the comparison of the traditional two-component model and a two-dimensional Gaussian distribution. Calculations based on the Gaussian distribution are presented and used to deduce shape distribution parameters from radar measurements.

20. DISTRIBUTION / AVAILABILITY OF ABSTRACT	21 ABSTRACT SECURITY CLASSIFICATION
☐ UNCLASSIFIED/UNLIMITED ☒ SAME AS RPT ☐ DTIC USERS	Unclassified

22a. NAME OF RESPONSIBLE INDIVIDUAL	22b TELEPHONE (Include Area Code)	22c OFFICE SYMBOL
James I. Metcalf	(617) 3774405	LYR

DD FORM 1473, 84 MAR 83 APR edition may be used until exhausted
All other editions are obsolete.

SECURITY CLASSIFICATION OF THIS PAGE
Unclassified

Reprinted from JOURNAL OF ATMOSPHERIC AND OCEANIC TECHNOLOGY, Vol. 5, No. 4, August 1988
American Meteorological Society

A New Slant on the Distribution and Measurement of Hydrometeor Canting Angles

JAMES I. METCALF

Air Force Geophysics Laboratory, Hanscom AFB, Massachusetts

(Manuscript received 31 August 1987, in final form 27 January 1988)

ABSTRACT

Several models have been developed in the past to describe the distribution of hydrometeor canting angles and the resulting effects on polarimetric radar measurements. These models are reviewed to compare their characteristics and to assess their validity under specified conditions. Of particular interest is the comparison of the traditional two-component model and a two-dimensional Gaussian distribution. Calculations based on the Gaussian distribution are presented and used to deduce shape distribution parameters from radar measurements.

1. Introduction

The distribution of canting angles is one of the microphysical attributes of hydrometeors that affect the polarization-dependent parameters measurable by radar and that may therefore be deduced from polarimetric radar measurements. Recent work on this subject has included some inconsistencies, unnecessary complications, and erroneous interpretations. The fundamental issues which need to be addressed in relation to hydrometeor canting angles are: (i) specification of a form of the canting angle distribution, both in one dimension and in two dimensions; and (ii) determination of reasonable values of the distribution parameters for various types of hydrometeors. In sections 2 and 3 we discuss key developments in the modeling of canting angle distributions and describe radar measurements which support theoretical results pertaining to the standard deviation of canting angles of raindrops. Concepts of a two-dimensional distribution of canting angles are discussed in section 4, and a comparison of the traditional two-component model and the two-dimensional Gaussian model is presented in section 5. Calculations based on the two-dimensional Gaussian model are used in section 6 to derive estimates of mean backscatter amplitude and power ratios from polarimetric radar measurements.

The angular parameters of hydrometeor canting are illustrated in Fig. 1. We use θ to denote the absolute canting angle, which is the angle between the local vertical and the hydrometeor symmetry axis, independent of azimuth. Following a long standing tradition, we use α to denote the apparent canting angle, which is the projection of θ onto a plane perpendicular to the line of sight. For convenience, most of the following discussion is based on the assumption that $\bar{\alpha} = 0$.

Corresponding author address: Dr. James Metcalf, AFGL/LYR, Hanscom Air Force Base, MA 01731.

2. Theory for the one-dimensional distribution

Beginning with the work of Saunders (1971) there has been a tradition of treating the canting angle distribution as one-dimensional in a plane perpendicular to the radar line of sight. McCormick and Hendry (1975) and others have adopted a two-component model of the apparent canting angle distribution in which one fraction of the hydrometeors has a single fixed apparent canting angle and the complementary fraction has a uniform random distribution. This model of the distribution function was used, for example, by Metcalf (1986) in the computation of polarization dependent parameters measurable in rain. McCormick and Hendry related the effective fraction of oriented scatterers ρ_α to a distribution function by the equation

$$\rho_\alpha = \int_{-\pi/2}^{+\pi/2} \cos 2(\alpha - \bar{\alpha}) p(\alpha - \bar{\alpha}) d(\alpha - \bar{\alpha}), \quad (1)$$

where $p(\alpha - \bar{\alpha})$ is the distribution function relative to the mean apparent canting angle $\bar{\alpha}$. They did not, however, specify the form of the distribution.

From the two-component model the reflectivity-weighted average of the complex backscatter amplitude ratio $ve^{j(\delta \pm 2\alpha)}$ defined for circular polarization is given by

$$\overline{ve^{j(\delta \pm 2\alpha)}} = \rho_\alpha \bar{v} e^{j(\bar{\delta} \pm 2\bar{\alpha})}, \quad (2)$$

(McCormick and Hendry 1975) where δ is the backscatter differential phase shift, ρ_α is given by Eq. (1), and the upper and lower signs denote the transmission of right and left circularly polarized signals, respectively. The quantity $ve^{j\delta}$ is approximately real for Ray-

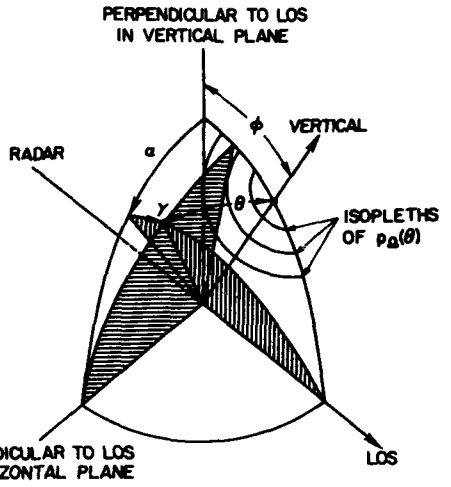

FIG. 1. Sector of the hemisphere on which p_α is defined, showing the radar elevation angle ϕ, the canting angle θ of the symmetry axis of a particle from the vertical, the projection α of the canting angle onto the plane perpendicular to the radar line of sight (LOS), and the angle γ of the symmetry axis from this plane.

leigh–Gans scatterers and is positive and negative for prolate and oblate spheroids, respectively. The effect of radar elevation angle on $\bar{\nu}$ is included through the assumption that for an individual hydrometeor the apparent amplitude ratio is given by $\nu_a = \nu_0 \cos^2\gamma$, where ν_0 is the amplitude ratio of the hydrometeor when viewed perpendicularly to its symmetry axis and γ is the angle of the symmetry axis from a plane perpendicular to the radar line of sight (see Fig. 1). If the average orientation of the symmetry axes is vertical, then $\bar{\gamma}$ is equal to the radar elevation angle ϕ and $\bar{\nu} = \bar{\nu}_0 \cos^2\phi$. Because the function $\cos 2\alpha$ passes through a full cycle in the interval $-\pi/2 \leq \alpha \leq \pi/2$, the randomly oriented fraction $(1 - \rho_\alpha)$ contributes nothing to the average in Eq. (2), and the effect of the apparent amplitude ratio is evident only in the elevation angle dependence of $\bar{\nu}$. The reflectivity-weighted average of the backscatter power ratio ν^2 is given by

$$\overline{\nu^2} = \overline{\nu_0^2}\left[\rho_\alpha \cos^4\phi + \left(\frac{8}{15}\right)(1 - \rho_\alpha)\right] \quad (3)$$

where the factor $^8/_{15}$ results from integrating the function $\cos^4\gamma$ over a hemisphere of solid angle. Equation (3) implies an ambiguity in the two-component model, as the distribution over a hemisphere is inconsistent with the idea of a one-dimensional canting angle in the plane perpendicular to the line of sight. Specifically, the quantity $\bar{\nu}$ in Eq. (2) is an average over a distribution of actual shapes, whereas the quantity ν^2 in Eq. (3) is an average over distributions of both actual and apparent shapes.

Beard and Jameson (1983) showed, on the basis of turbulence theory, that a Gaussian distribution of velocity fluctuations would yield a Gaussian distribution of the tangent of the apparent canting angle, from which one can derive $p(\alpha)$. [There is an error in their equation defining $p(\alpha)$, in that the argument of the exponential function should be $-\tan^2\alpha/(2\sigma^2_{\tan\alpha})$, using the present notation.] Their calculations showed that the standard deviation σ_α of the apparent canting angle is less than 4° for a thunderstorm raindrop size distribution and turbulent energy dissipation rates up to 0.2 $m^2 s^{-3}$. For small standard deviations of apparent canting angle, the differences between a Gaussian distribution of α and a Gaussian distribution of $\tan\alpha$ are slight. However, for large values of the standard deviation, the Gaussian distribution of $\tan\alpha$ yields unrealistic results, as it does not yield a uniform distribution as $\sigma_{\tan\alpha}$ approaches infinity and it yields zero probability density at $\alpha = \pm\pi/2$ for all values of $\sigma_{\tan\alpha}$. It is therefore useful to consider the properties of a Gaussian distribution of the apparent canting angle. Hendry et al. (1976) and Torlaschi et al. (1984) used such a distribution but truncated it at $\pm\pi/2$ to reflect the fact that the distribution is physically limited to this interval. The resulting relationship of σ_α to ρ_α is

$$\rho_\alpha = \exp(-2\sigma_\alpha^2)\,\mathrm{Re}\{\mathrm{erf}[\pi/(2\sqrt{2}\sigma_\alpha) + i\sqrt{2}\sigma_\alpha]\} \quad (4)$$

where σ_α is expressed in radians. Metcalf and Ussailis (1984) suggested that the distribution in the interval $\pm\pi/2$ could be viewed as a summation of segments of an infinite Gaussian distribution folded back on itself within this interval, i.e.,

$$p(\alpha) = (\sqrt{2\pi}\sigma_\alpha)^{-1} \sum_{n=-\infty}^{+\infty} \exp[-(\alpha + n\pi)^2/(2\sigma_\alpha^2)]. \quad (5)$$

Because the function $\cos 2\alpha$ is cyclical in this interval, the limits of integration in Eq. (1) can be extended to infinity, with the result that

$$\rho_\alpha = \exp(-2\sigma_\alpha^2) \quad (6)$$

which is the asymptotic limit of Eq. (4) for small σ_α. The approach of Metcalf and Ussailis also yields the aesthetically satisfying result that $dp(\alpha)/d\alpha = 0$ at $\alpha = \pm\pi/2$.

It should be noted that *neither* in the approach of Hendry et al. and Torlaschi et al., nor in the approach of Metcalf and Ussailis is the parameter σ_α of the Gaussian distribution function exactly equal to the standard deviation of the apparent canting angle distribution defined on the finite interval from $-\pi/2$ to $+\pi/2$. The latter, denoted by $\hat{\sigma}_\alpha$, approaches the former at small values of σ_α, but as σ_α approaches infinity, the resulting uniform distribution on the finite interval yields a standard deviation of $\pi/\sqrt{12}$ radians, or about 52°. Hence it may be preferable to use ρ_α

rather than σ_α as the primary descriptor of the orientation state of a backscatter medium.

3. Measurements

Hendry et al. (1987) developed a method of deriving a canting parameter from measurements with varying linear polarization. They showed that measurement of the maximum and minimum linear cross-polarized power as the linear polarization vector is rotated through at least 180° yields the parameter

$$\rho_4 = \int_{-\pi/2}^{+\pi/2} \cos 4(\alpha - \bar{\alpha}) p(\alpha - \bar{\alpha}) d(\alpha - \bar{\alpha}), \quad (7)$$

defined on the basis of a one-dimensional distribution of apparent canting angle, which differs from ρ_α, defined by Eq. (1), only by the coefficient of the argument of the cosine. The relation of ρ_4 to ρ_α depends on the distribution function. The two-component model yields $\rho_4 = \rho_\alpha$, and a one-dimensional Gaussian distribution function yields $\rho_4 = \rho_\alpha^4$. Two other distribution functions, triangular and rectangular, which seem less realistic than the Gaussian, yield relations of ρ_4 and ρ_α that differ only slightly from that of the Gaussian. The distinction between ρ_4 as a measurable parameter of the canting angle distribution and ρ_α as a conceptual parameter highlights the importance of specifying a physically realistic canting angle distribution for the purpose of interpreting radar measurements. Measurements by Hendry et al. in rain yielded $\rho_4 = 0.914$, which implies $\sigma_\alpha = 6.1°$ for a Gaussian distribution. This value is comparable to the theoretical value deduced by Beard and Jameson.

4. Theory for the two-dimensional distribution

The effect of canting out of the plane perpendicular to the radar line of sight has until recently been included implicitly with the effect of a distribution of hydrometeor shapes, as might result from raindrop oscillation or from the presence of multiple types of hydrometeors. Recent efforts (Jameson 1987) have been undertaken to analyze two-dimensional canting relative to the local vertical, with the goals of (1) correctly separating the effects of shape distribution from the effects of canting angle distribution and (2) explicitly describing the apparent changes of canting and shape distributions in radar observations at nonzero elevation angles. The two-dimensional distribution, defined on a hemispherical surface, must be represented by a probability density per unit solid angle, here denoted by p_Ω. The distribution is assumed to have a maximum value at a single direction, typically near the vertical, and to be axisymmetric about the direction of the maximum. If the maximum of p_Ω is at the vertical, then p_Ω can be expressed as a function of θ only. If the maximum of p_Ω is displaced from the vertical, as might occur as a result of wind shear or electric field, then the distribution is not a function of θ alone but can be expressed as a function of a subsidiary coordinate relative to the location of the maximum. For convenience in the computations to be discussed in section 5, we assume the maximum of p_Ω to be at the vertical. The angular coordinates pertinent to this distribution are illustrated in Fig. 1. Here the symmetry axis of a hydrometeor lies at an angle θ from the vertical, projects an angle α on the plane perpendicular to the line of sight, and lies at an angle γ from that plane. If $\bar{\alpha} = 0$, the effects of nonzero value of $\bar{\gamma}$ are equivalent to the effects of a nonzero radar elevation angle ϕ. A nonzero mean apparent canting angle, i.e., $\bar{\alpha} \neq 0$, affects the angular argument of certain radar-measurable parameters but does not affect the magnitudes of the quantities discussed below.

The two-dimensional distribution of θ yields the one-dimensional distribution of α by the relation

$$p(\alpha) = \int_{-\pi/2}^{+\pi/2} p_\Omega(\theta(\alpha, \gamma)) \cos\gamma d\gamma \quad (8)$$

where the angles are related by

$$\cos\theta = \cos\alpha \cos\phi \cos\gamma + \sin\phi \sin\gamma. \quad (9)$$

A two-dimensional Gaussian distribution

$$p_\Omega(\theta) = (2\pi\sigma_\theta^2)^{-1} \exp[-\theta^2/(2\sigma_\theta^2)] \quad (10)$$

is particularly advantageous, as it yields a Gaussian distribution of α with $\sigma_\alpha = \sigma_\theta$. Jameson (1987) used a two-dimensional Gaussian distribution in calculating radar-measurable parameters, but the utility of his results is diminished by his arbitrary selection of $\sigma_\theta = 18°$, which is much larger than the values deduced by Beard and Jameson (1983) or implied by the measurements of Hendry et al. (1987). Jameson also presented results based on a one-dimensional Gaussian distribution of θ. Aside from the conceptually dubious merit of applying a one-dimensional distribution function to a two-dimensionally distributed variable, the practical value of such a distribution function is uncertain at best, as it yields a singularity of the probability density per unit solid angle at $\theta = 0$, does not yield spherical uniformity as $\sigma_\theta \to \infty$, and does not yield simple relationships between $p_\Omega(\theta)$ and $p(\alpha)$ or among σ_θ, $\hat{\sigma}_\alpha$ and ρ_α.

5. Comparison of canting angle models

a. Formulation

Calculations have been performed with the two-dimensional Gaussian distribution to compare this model with the two-component model described in section 2 and to determine the relationship of $p_\Omega(\theta)$ to $p(\alpha)$, the effects of truncating the distribution, the mean values of backscatter amplitude and power ratios, the circular polarization cross correlation measurable by radar, and

the correct normalization of the Gaussian distribution defined on a spherical surface. The distribution within the domain $0 \leq \theta \leq \pi/2$ was approximated successively by Eq. (10), by

$$p_\Omega(\theta) = (2\pi\sigma_\theta^2)^{-1}\{\exp[-\theta^2/(2\sigma_\theta^2)] + \exp[-(\theta - \pi)^2/(2\sigma_\theta^2)]\} \quad (11)$$

and by

$$p_\Omega(\theta) = (2\pi\sigma_\theta^2)^{-1} \sum_{n=-2}^{+1} \exp[-(\theta + n\pi)^2/(2\sigma_\theta^2)]. \quad (12)$$

Within the finite domain, Eq. (10) represents a Gaussian distribution truncated at $\theta = \pi/2$. Equation (11) represents a Gaussian distribution truncated at $\theta = \pi$ and folded back on itself at $\theta = \pi/2$. Equation (12) represents a Gaussian distribution truncated at $\theta = 2\pi$ and quadruply folded back on itself in the interval $0 \leq \theta \leq \pi/2$. The successive approximations were used to assess the effects of truncation and to assure accurate results as σ_θ increased.

We assume that the apparent amplitude ratio is given by $\nu_a(\gamma) = \nu_0 \cos^2\gamma$, as in section 2. For comparison of the two distribution models, it is convenient to define the amplitude ratio factor

$$f_A(\sigma_\theta) = \bar{\nu}_a/\nu_0 = \overline{\cos^2\gamma \cos 2\alpha} \quad (13)$$

and the power ratio factor

$$f_P(\sigma_\theta) = \overline{\nu_a^2}/\nu_0^2 = \overline{\cos^4\gamma}. \quad (14)$$

For comparison with the measurements of Hendry et al., we use their formulation to define the quantity

$$\rho_{4G} = [\overline{(\nu_a^2/\nu_0^2)\cos 4\alpha}]/(\overline{\nu_a^2}/\nu_0^2) = \overline{\cos^4\gamma \cos 4\alpha}/\overline{\cos^4\gamma} \quad (15)$$

which is, for a two-dimensional canting angle distribution, the analog of ρ_4, defined in Eq. (7). The overbar in Eqs. (13), (14), and (15) denotes averaging over a hemisphere weighted by the distribution function p_Ω. The form of ρ_{4G} differs from that of ρ_4 because the distribution function $p_\Omega(\theta)$ jointly affects both the apparent canting, which is specified by α, and the apparent shape, which is dependent on γ. Hendry et al. (1987), in developing the parameter ρ_4, separated the average of ν^2 from the average of $\cos 4\alpha$. Using a two-dimensional distribution function, with the traditional assumption that the shape and orientation distributions are independent, we factor the parameter ν^2 into two averages, one over the distribution of actual shapes and one over the distribution of apparent shapes. In this case it is the average of ν^2 over the distribution of actual shapes which is canceled out of the ratio of maximum to minimum linear cross polarized received power, and the measurements can be shown to yield ρ_{4G}, defined in Eq. (15), rather than ρ_4, defined in Eq. (7).

In a backscatter medium comprising particles of a common shape, the two-component model yields the amplitude ratio factor

$$f_A = \rho_\alpha \cos^2\phi \quad (16)$$

and the power ratio factor

$$f_P = \rho_\alpha \cos^4\phi + \left(\frac{8}{15}\right)(1 - \rho_\alpha) \quad (17)$$

corresponding to Eq. (3).

b. Calculations

The results corresponding to a radar elevation angle of zero and particles of a common shape are summarized in Table 1. The calculations show that at small to moderate values of σ_θ, the two-dimensional Gaussian distribution of θ yields a nearly Gaussian distribution of α, with $\hat{\sigma}_\alpha \approx \sigma_\theta$. As σ_θ increases, $\hat{\sigma}_\alpha$ approaches its asymptotic limit, as discussed in section 2. Truncation effects, not documented in Table 1, are evident only if the truncation point is less than about $3.5\sigma_\theta$. In other words, Eq. (10) is a valid approximation for $\sigma_\theta \leq 25°$ and Eq. (11) is valid for $\sigma_\theta \leq 50°$. Equation (12) should be valid for $\sigma_\theta \leq 100°$, at which value $p(\alpha)$ varies by only 0.6% between 0 and $\pi/2$. The selection of one of these three equations to approximate the Gaussian model in the present calculations is dictated by the magnitude of σ_θ. All yield identical results if $\sigma_\theta \leq 25°$; Eqs. (11) and (12) are equally usable if $\sigma_\theta \leq 50°$.

At zero elevation angle the amplitude and power ratio factors calculated from the Gaussian model are smaller than the respective factors calculated from the two-component model. (Note that the parameter ρ_α *is* the amplitude ratio factor for the two-component model.) This results from integrating over the hemisphere, i.e., both in α and in γ, and reflects the decrease of the functions $\cos^2\gamma$ and $\cos^4\gamma$ as γ deviates from zero. The calculated amplitude and power ratio factors for several elevation angles are shown in Figs. 2 and 3. The amplitude ratio factor based on the Gaussian model is well fit by the function

$$f_A = \exp(-3\sigma_\theta^2)\cos^2(\phi) \quad (18)$$

for $\sigma_\theta \leq 40°$. The power ratio factor at $\phi = 0°$ is fairly well fit by the function

$$f_P = \exp(-4\sigma_\theta^2) + \left(\frac{8}{15}\right)[1 - \exp(-4\sigma_\theta^2)]. \quad (19)$$

One is tempted to model the power ratio factor by

$$f_P = \exp(-4\sigma_\theta^2)\cos^4\phi + \left(\frac{8}{15}\right)[1 - \exp(-4\sigma_\theta^2)]. \quad (20)$$

However, for $\phi \geq 20°$ this formula is a less accurate approximation to the calculated values than is Eq. (17). Therefore, for purposes of interpreting radar measurements it may be preferable to use a value of the power ratio factor calculated from the Gaussian model rather

TABLE 1. Integrated parameters calculated from two-dimensional Gaussian distribution of absolute canting angle. Calculations pertain to spheroidal scatterers with mean vertical orientation of symmetry axes, viewed at horizontal incidence (zero elevation angle).

σ_θ (deg)	$\hat{\sigma}_a$ (deg)	ρ_a	$\bar{\nu}_a/\nu_0$ (Gauss)	$\overline{\nu_a^2}/\nu_0^2$ Gauss	$\overline{\nu_a^2}/\nu_0^2$ 2-component	ρ_c Gauss	ρ_c 2-component
5	5.006	0.985	0.977	0.985	0.993	0.985	0.988
10	10.05	0.940	0.912	0.944	0.972	0.939	0.954
15	15.18	0.869	0.816	0.887	0.939	0.867	0.897
20	20.46	0.775	0.700	0.825	0.895	0.771	0.819
30	31.44	0.544	0.457	0.713	0.787	0.542	0.613
40	40.65	0.323	0.261	0.633	0.684	0.328	0.390
50	46.34	0.169	0.135	0.585	0.612	0.177	0.216
60	49.36	0.080	0.064	0.550	0.571	0.086	0.105
80	51.53	0.014	0.011	0.531	0.540	0.015	0.010

than to use the analytical approximations of Eqs. (19) and (20).

For backscatter from particles of a common shape, the two-component model yields a circular polarization cross correlation given by

$$\rho_c = \rho_a \cos^2\phi \Big/ \left[\rho_a \cos^4\phi + \left(\frac{8}{15}\right)(1-\rho_a)\right]^{1/2}. \quad (21)$$

The cross correlation from the Gaussian model is the ratio of the integrated parameters $\bar{\nu}_a/\nu_0$ and $(\overline{\nu_a^2}/\nu_0^2)^{1/2}$. As shown in Table 1, it is consistently lower than that derived from the two-component model, except at $\sigma_\theta = 80°$.

In general, the integral of $p_\Omega(\theta)$, defined in Eqs. (10), (11), and (12), over a hemisphere should yield a value less than unity. This is due to the fact that for a given value of θ, the incremental area on the hemisphere, given by $\sin\theta d\theta d\zeta$, is less than the incremental area on a plane, given by $\theta d\theta d\zeta$, where θ is a colatitudinal or radial coordinate and ζ is a longitudinal or azimuthal coordinate. As σ_θ increases, the distribution is spread to regions of larger θ, where the area effect is more significant, and we find that the integral yields a value approximately equal to $\exp(-0.30\sigma_\theta^2)$, with σ_θ in radians. All of the quantities derived from the Gaussian distribution and shown in Table 1 or in Figs. 2 and 3 are normalized by the magnitude of the integral of the probability density function.

c. *Prolate spheroids*

The foregoing theory and calculations apply to spheroidal hydrometeors of any ellipticity, provided

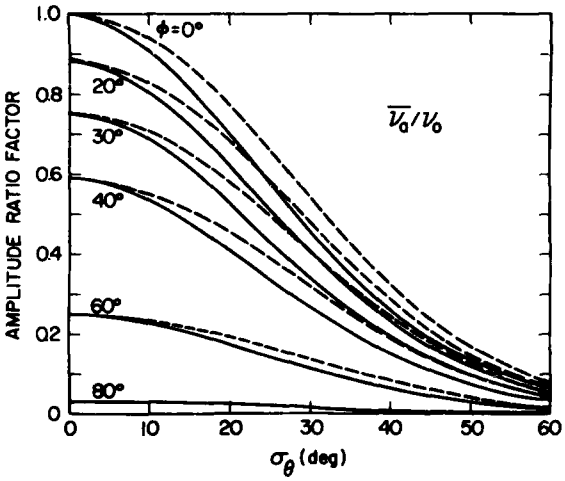

FIG. 2. Amplitude ratio factor $\bar{\nu}_a/\nu_0$ as a function of standard deviation of canting angles with radar elevation angle ϕ as a parameter. Solid and broken lines denote calculations from the Gaussian and two-component models, respectively.

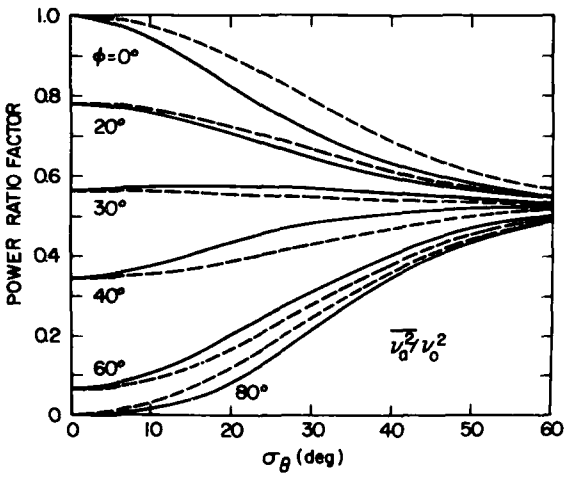

FIG. 3. Power ratio factor $\overline{\nu_a^2}/\nu_0^2$ as a function of standard deviation of canting angles with radar elevation angle ϕ as a parameter. Solid and broken lines denote calculations from the Gaussian and two-component models, respectively. At an elevation angle of 31.3° in the two-component model the power ratio factor is independent of σ_θ. In the Gaussian model the elevation angle at which this factor equals its asymptotic value $^8/_{15}$ varies slightly with σ_θ.

that they have a *single* most probable orientation angle. Prolate spheroids under the sole influence of aerodynamic forces tend to be oriented with their symmetry axes horizontal but uniformly distributed in azimuth. The appropriate distribution in this case is one having a minimum at $\theta = 0$ and a maximum at $\theta = \pi/2$, i.e., at the edge of the hemisphere. The resulting value of f_A is negative, due to the dominant contribution of the $\cos 2\alpha$ factor in Eq. (13) when α is near $\pi/2$. Because the complex backscatter amplitude ratio $ve^{j(\delta \pm 2\alpha)}$ is positive for vertically oriented prolate spheroids, the average of this ratio over a distribution of nearly horizontal orientations is negative. This is consistent with the fact that horizontally oriented prolate spheroids appear similar to vertically oriented oblate spheroids, for which f_A is positive and $ve^{j\delta}$ is negative. The distribution of prolate spheroids was modeled in the interval $0 \leq \theta \leq \pi/2$ by the function

$$p_\Omega(\theta) = (2\pi\sigma_\theta^2)^{-1} \exp[-(\theta - \pi/2)^2/(2\sigma_\theta^2)]. \quad (22)$$

Calculations corresponding to zero radar elevation angle are illustrated in Table 2. In this case the asymptotic value of $|f_A|$ is 0.5 as $\sigma_\theta \to 0$ and that of f_P is 0.375; these are the averages of $\cos^2\gamma$ and $\cos^4\gamma$, respectively. For these calculations the quantity $\hat{\sigma}_\alpha$ is redefined to represent the standard deviation of the apparent vertically oriented oblate spheroids. The parameter ρ_α is similarly redefined. The relation of ρ_α and $\hat{\sigma}_\alpha$ is similar to that in the case of oblate spheroids. Because of the broad azimuthal distribution in the present case, $\hat{\sigma}_\alpha$ is much larger than σ_θ when σ_θ is small. As σ_θ increases, $\hat{\sigma}_\alpha$ approaches the same limit as for oblate spheroids. The amplitude ratio factor f_A is significantly less than ρ_α in this case because of the wide distribution of symmetry axes in the γ coordinate. The power ratio factor f_P increases with σ_θ to approach its asymptotic value of 0.533. Application of the two-component model to horizontally oriented prolate spheroids yields the amplitude ratio factor

$$f_A = -\left(\frac{1}{2}\right)\rho_\alpha \cos^2\phi \quad (23)$$

and the power ratio factor

$$f_P = \left(\frac{3}{8}\right)\rho_\alpha \cos^4\phi + \left(\frac{8}{15}\right)(1 - \rho_\alpha) \quad (24)$$

which yield the cross correlation shown in Table 2. The respective factors ½ and ⅜ result from the fact that in this case the "oriented fraction" is distributed uniformly in azimuth.

6. Application of the two-dimensional model

The quantities f_A and f_P enable the estimation of the reflectivity-weighted mean and mean square of the actual amplitude ratio of a distribution of hydrometeors from measurements of the cross covariance amplitude ratio (CCAR $\equiv W/W_2$ in the notation of McCormick and Hendry 1975) and the circular depolarization ratio (CDR), respectively, if a parameter of the canting angle distribution is measurable separately. For Rayleigh–Gans scatterers the mean actual amplitude ratio is given by

$$|\bar{\nu}_0| = |\text{CCAR}|/f_A = |\text{ORTT}|(\text{CDR})^{1/2}/f_A \quad (25)$$

where ORTT, in the notation of Hendry et al. (1976, 1987), is the measured cross correlation between the two received signals. The mean square actual amplitude ratio is given by

$$\overline{\nu_0^2} = \text{CDR}/f_P \quad (26)$$

where the elevation angle dependence of the measured parameters is incorporated in the values of f_A and f_P. Equations (25) and (26) incorporate the traditional assumption that the shape and orientation distributions are independent. As used here, f_A and f_P are weighted only by the probability density ρ_Ω, assumed to be size-independent, while $\bar{\nu}_0$ and $\overline{\nu_0^2}$ are weighted by the number density and backscatter cross section as functions of hydrometeor size. The variance of the actual amplitude ratio is $\sigma_\nu^2 = \overline{\nu_0^2} - \bar{\nu}_0^2$.

The results shown in Table 3 are based on the published data of Hendry et al. (1987). Their parameter

TABLE 2. Integrated parameters calculated from two-dimensional Gaussian distribution of absolute canting angle. Calculations pertain to prolate spheroidal scatterers with mean horizontal orientation of symmetry axes, viewed at horizontal incidence (zero elevation angle).

σ_θ (deg)	$\hat{\sigma}_\alpha$ (deg)	ρ_α	$\bar{\nu}_a/\nu_0$ (Gauss)	$\overline{\nu_a^2}/\nu_o^2$ Gauss	$\overline{\nu_a^2}/\nu_o^2$ 2-component	ρ_c Gauss	ρ_c 2-component
1	7.95	0.972	−0.500	0.375	0.379	−0.816	−0.789
3	13.78	0.917	−0.496	0.376	0.388	−0.809	−0.736
5	17.77	0.862	−0.489	0.377	0.397	−0.796	−0.684
10	25.02	0.728	−0.457	0.383	0.418	−0.738	−0.563
15	30.39	0.605	−0.410	0.394	0.438	−0.654	−0.457
20	34.66	0.495	−0.355	0.408	0.455	−0.556	−0.367
30	40.89	0.325	−0.249	0.441	0.482	−0.376	−0.234
40	44.69	0.216	−0.172	0.468	0.499	−0.251	−0.153
50	46.95	0.150	−0.121	0.486	0.510	−0.174	−0.105
60	48.31	0.110	−0.090	0.498	0.516	−0.127	−0.077

TABLE 3. Hydrometeor shape distribution parameters derived from radar measurements of Hendry et al. (1987).

	Case			
	1	2	3	
	Precipitation type			
	Heavy rain 6 Jul 84	Melting layer 10 Nov 84	Snow 4 Mar 85	
Elevation angle (deg)	4.7	16.3	7.0	
ρ_4 (Measured)	0.914	0.607	0.280	
|CCAR| (Measured)	0.179	0.0139	0.0222	
CDR (Measured)	0.0422	0.00158	0.00631	
			oblate	prolate
σ_θ (Present model)	6.0°	13.7°	22.4°	20.0°
f_A	0.961	0.777	0.631	−0.350
f_P	0.966	0.793	0.783	0.413
$\bar{v}_0 e^{i\bar{\delta}}$	−0.187	−0.0179	−0.0353	0.0634
$\overline{v_0^2}$	0.0436	0.00200	0.00806	0.0153
σ_v	0.0941	0.0410	0.0826	0.106

ρ_4, reinterpreted here as ρ_{4G}, yields a value of σ_θ through the two-dimensional Gaussian model. Successive calculations with different values of σ_θ were used to determine the particular value of σ_θ that yields the measured value of ρ_{4G}. This value of σ_θ, in turn, yields values of f_A and f_P to be used in Eqs. (25) and (26). Case 1, an observation of heavy rain, yields a mean amplitude ratio equal to that of raindrops of 0.73 axial ratio, which corresponds to 4.6 mm equivalent spherical diameter with a Pruppacher-Pitter size-shape relation. The standard deviation σ_v, equal to about half the magnitude of the mean $\bar{v}_0$ in this case, implies that essentially all the hydrometeors are of oblate shape, which is to be expected in rain. Each of cases 2 and 3 yields σ_v greater than the magnitude of $\bar{v}_0 e^{i\bar{\delta}}$. Case 2 is an observation of a melting layer, and the data used for the present analysis are from near its base, about 200 m below the altitude of the maximum circular depolarization ratio. At this altitude the hydrometeors are likely to be at least partially melted, but the larger derived value of σ_θ and smaller values of other parameters, compared to those of case 1, imply that the hydrometeors cannot be approximated by a single distribution of oblate spheroids. Case 3, an observation of snow, yields potentially ambiguous results because of a nonzero mean canting angle and because of the more likely role of prolate spheroidal scatterers. The radar measurements yielded $\bar{\alpha} = 10°$, and the component of canting relative to the plane perpendicular to the line of sight, although unknown, may be of comparable magnitude. Hence, at the radar elevation angle of 7°, $\bar{\gamma}$ may lie between −3° and 17°, and the measured value of ρ_{4G} corresponds to σ_θ between 21.8° (at $\gamma = 17°$) and 22.5° (at $\gamma = 0°$) for oblate spheroids. The tabulated quantities for Case 3 are based on the assumption that $\bar{\gamma} = 7°$. Calculations for oblate and prolate spheroids are shown for comparison. The transposition of signs of the quantities f_A and $\bar{v}_0 e^{i\bar{\delta}}$ between the two interpretations indicates that in either case the average horizontal dimension of the scatterers is greater than the average vertical dimension. The standard deviation σ_v exceeds the magnitude of $\bar{v}_0 e^{i\bar{\delta}}$ by a smaller factor in the prolate case than in the oblate, suggesting that the prolate description is somewhat better than the oblate, although neither is fully satisfactory.

For either oblate or prolate hydrometeors, one can hypothesize a distribution having a relatively large number of nearly spherical shape and a relatively small number of highly nonspherical shape, which would yield a small magnitude of $\bar{v}_0 e^{i\bar{\delta}}$ and a relatively large value of σ_v. Such a distribution, requiring that all the hydrometeors be either oblate or prolate, seems less realistic than a mixture of oblate and prolate shapes, the analysis of which is beyond the scope of this paper. Measurements of cloud physical parameters by airborne instruments are essential to the development of realistic shape distributions but were unavailable in these cases. In evaluating cases 2 and 3, one must realize that the real part of the amplitude ratio $ve^{i(\delta \pm 2\alpha)}$ is a bipolar function, being positive if the larger apparent dimension of a spheroid is vertical and negative if it is horizontal. Hence, a combination of shape and orientation distributions may yield a magnitude of $\bar{v}_0 e^{i\bar{\delta}}$ much less than the standard deviation σ_v. It is likely that the shape and orientation distributions are not independent, contrary to the traditional assumption. It is possible that the approximation $v_a = v_0 \cos^2\gamma$ may not be generally valid for ice phase hydrometeors. Finally, the role of propagation effects, unknown in these

cases, must be considered in the proper interpretation of polarimetric radar measurements.

7. Conclusion

The derivation of canting angle parameters from radar measurements is an essential element of characterization of hydrometeor types. As polarimetric meteorological radar techniques become more comprehensive and more quantitative it is desirable that the underlying theory become more realistic while maintaining simplicity of form. Because of its advantages and simplicity, the Gaussian distribution of canting angles (both one-dimensional and two-dimensional) seems to be a desirable standard until such time as there is a strong rationale for using an alternative distribution. Theory and measurements indicate that the standard deviation of canting angles of raindrops is typically about 4°–6°. Differences in amplitude and power ratio factors derived from the Gaussian and two-component models are small enough in some cases that they do not substantially affect calculations such as those of Metcalf (1986). On the other hand, the differences are large enough to justify the use of the Gaussian model in preference to the two-component model in the interpretation of radar measurements.

In this and all previous work on this subject, authors have assumed the independence of canting angle distribution and particle shape distribution. This assumption permits separation of the respective physical parameters, e.g., $\bar{\alpha}$, ρ_α and $\bar{\nu}_0$. In practice, since the distributions of canting angle and of shape are likely to be size-dependent, the respective parameters are likely to be correlated. Future efforts must address this more complicated analytical problem.

Acknowledgments. I am grateful to Dr. Alan Bohne of AFGL, to Mr. Archibald Hendry (retired from the National Research Council of Canada), to Dr. Arthur Jameson of Applied Research Corp., and to an anonymous reviewer for their help in the refinement and presentation of these ideas.

REFERENCES

Beard, K. V., and A. R. Jameson, 1983: Raindrop canting. *J. Atmos. Sci.*, **40**, 448–454.

Hendry, A., G. C. McCormick and B. L. Barge, 1976: The degree of common orientation of hydrometeors observed by polarization diversity radars. *J. Appl. Meteor.*, **15**, 633–640.

——, Y. M. M. Antar and G. C. McCormick, 1987: On the relationship between the degree of preferred orientation in precipitation and dual-polarization radar echo characteristics. *Radio Sci.*, **22**, 37–50.

Jameson, A. R., 1987: Relations among linear and circular polarization parameters measured in canted hydrometeors. *J. Atmos. Oceanic Technol.*, **4**, 634–645.

McCormick, G. C., and A. Hendry, 1975: Principles for the radar determination of the polarization properties of precipitation. *Radio Sci.*, **10**, 421–434.

Metcalf, J. I., 1986: Interpretation of the autocovariances and cross-covariance from a polarization diversity radar. *J. Atmos. Sci.*, **43**, 2479–2498.

——, and J. S. Ussailis, 1984: Radar system errors in polarization diversity measurements. *J. Atmos. Oceanic Technol.* **1**, 105–114.

Saunders, M. J., 1971: Cross polarization at 18 and 30 GHz due to rain. *IEEE Trans. Antennas Propag., AP-19*, 273–277.

Torlaschi, E., R. G. Humphries and B. L. Barge, 1984: Circular polarization for precipitation measurement. *Radio Sci.*, **19**, 193–200.